Journal of Organic and Pharmaceutical Chemistry

Review Article

OPEN ACCESS
Freely available online on
http://ophcj.nuph.edu.ua

UDC 54.057:547.833:615.2

M. A. Jordaan, O. Ebenezer

Department of Chemistry, Faculty of Natural Sciences, Mangosuthu University of Technology,
511 Griffiths Mxenge Highway, 4031 Umlazi, South Africa

Biological Activities of Tetrahydroisoquinolines Derivatives

Abstract

1,2,3,4-Tetrahydroisoquinoline (THIQ) is a common scaffold of many alkaloids isolated from several plants and mammalian species. THIQ derivatives possess a broad spectrum of biological activities, including antitumor, antitubercular, antitrypanosomal, antibacterial, anti-HIV, anti-inflammatory, anti-Alzheimer, and anticonvulsant ones.

Aim. To cover updated studies on the biological properties of THIQ derivatives, as well as their structure-activity relationship (SAR), in order to highlight the effect of diverse functional groups responsible for the manifestation of the desired activity.

Results and discussion. We have presented the review on biological activities of THIQ. The SAR studies show that the electron-donating, electron-withdrawing and some heterocyclic functional groups on the backbone plays a vital role in modulating the biological potential of the compounds synthesized.

Conclusions. This review will help pharmaceutical researchers to synthesize novel and potent compounds containing THIQ scaffold.

Keyword: tetrahydroisoquinoline; assessment of biological activity; structure-activity relationship; molecular docking

М. А. Джордаан, О. Ебенезер

Кафедра хімії, Факультет природничих наук, Технологічний університет Мангосуту,
Шосе Гріффітс Мксенге, 511, Умлазі, 4031, Південно-Африканська Республіка

Біологічна активність похідних тетрагідроізохіноліну

Анотація

1,2,3,4-Тетрагідроізохінолін (ТГІХ) є розповсюдженим каркасом багатьох алкалоїдів, виділених з кількох видів рослин і ссавців. Похідні ТГІХ мають широкий спектр біологічних активностей, зокрема протипухлинну, протитуберкульозну, протитрипаносомну, антибактеріальну, анти-ВІЛ, протизапальну, протисудомну дію, а також є перспективними агентами для лікування хвороби Альцгеймера.

Мета. Цей огляд охоплює оновлені дослідження з біологічних властивостей похідних ТГІХ, а також взаємозв'язок між їхньою структурою та активністю (SAR), щоб підкреслити вплив різноманітних функціональних груп, відповідальних за прояв бажаної активності.

Результати та їх обговорення. У роботі наведено огляд біологічної активності ТГІХ. SAR дослідження свідчать, що електронодонорні, електроноакцепторні та деякі гетероциклічні функціональні групи, зв'язані з каркасом ТГІХ, відіграють дуже важливу роль у модулюванні біологічного потенціалу синтезованих сполук.

Висновки. Цей огляд допоможе дослідникам у галузі фармацевтики синтезувати нові та ефективні сполуки, що містять базову структуру ТГІХ.

Ключові слова: тетрагідроізохінлолін; оцінка біологічної активності; зв'язок структура-активність; молекулярний докінг

Citation: Jordaan, M. A.; Ebenezer, O. Biological Activities of Tetrahydroisoquinolines Derivatives. *Journal of Organic and Pharmaceutical Chemistry* **2023**, *21* (1), 20–38.
https://doi.org/10.24959/ophcj.23.268358
Received: *5 December 2022*; **Revised:** *26 February 2023*; **Accepted:** *26 March 2023*

Funding: The authors received no specific funding for this work.
Conflict of interests: The authors have no conflict of interests to declare.

ISSN 2308-8303 (Print) / 2518-1548 (Online)

Introduction

1,2,3,4-Tetrahydroisoquinoline (THIQ) is a common scaffold of many alkaloids isolated from several plants and mammalian species. Several synthetic routes for the synthesis of substances that could be incorporated as privileged structural motifs into therapeutic compounds have been reported, and this has led to outstanding advances in drug discovery. Although most of the general methods for the synthesis of THIQ involve with the metal-catalyzed hydrogenation of isoquinolines [1], THIQ possesses a broad spectrum of biological activities, including antitumor, antitubercular, antitrypanosomal, antibacterial, anti-HIV, anti-inflammatory, anti-Alzheimer, and anticonvulsant ones [2–9]. Some of the naturally occurring THIQ-based compounds and clinically available THIQ drugs, such as quinapril, noscapine, tubocurarine (one of the quaternary ammonium muscle relaxants), and apomorphine, are shown in Figure 1. Examples of clinical drugs containing 4-substituted THIQ include nomifensine and diclofensine. Nomifensine is a bicyclic antidepressant, and its powerful inhibitory effect on the dopamine uptake makes the drug have a distinct pharmacological profile different from that of tricyclic drugs [10]. The drug was withdrawn from the market due to the large number of reported cases of acute hemolytic anemia with intravascular hemolysis. The continued use of the drug required a new strategy to reduce the dose and increase its effectiveness. *Kang and coworkers* reported that nomifensine optimized by ionizing radiation (IR)-NF could enhance the therapeutic effectiveness in obstructing breast cancer proliferation by inducing cell death [11]. Diclofensine (Ro-8-4650) is an effective monoamine reuptake inhibitor, blocking the uptake of dopamine, noradrenaline, and serotonin by rat brain synaptosomes with IC_{50} values of 0.74, 2.3, and 3.7 nM, respectively. In addition, diclofensine binds to adrenergic, dopamine, serotonin, and trace amine-associated receptors [12]. This review, therefore, aims to present an updated information on the biological properties of THIQ derivatives and their structure-activity relationship (SAR) in order to highlight the effect of diverse functional groups responsible for the manifestation of the desired activity.

Results and discussion

Orexin receptor antagonists

Orexins (hypocretins) have been reported in the literature as endogenous compounds for two orphan G-protein-coupled receptors in the lateral hypothalamic area. Orexins can initiate orexin neurons, monoaminergic and cholinergic neurons to conserve an extensive, consolidated awake period in the hypothalamus/brainstem regions, [13, 14]. The orexin receptor stimulus is primarily excitatory and releases various neurotransmitters responsible for maintaining arousal, wakefulness, and appetite. Currently, three orexin receptor antagonists, namely, suvorexant, lemborexant, and daridorexant, are FDA approved for the treatment of insomnia. Several THIQ derivatives have been reported as orexin antagonists. ACT-335827, a phenylglycine-amide-substituted THIQ derivative, was reported by *Actelion and coworkers* as potent and OX_1 selective (**1**, IC_{50} OX_1 = 6 nM and OX_2 = 417 nM) [15]. RTIOX-276, **2** blocked the development of the locomotor sensitization to cocaine in rats and thereby reduced cravings for cocaine [16, 17] (Figure 2).

Watanabe and coworkers designed novel tetrahydroisoquinoline derivatives with a fluoroethyl group and evaluated their effectiveness for positron emission tomography (PET) imaging of OX_1R [18]. To quantify the affinity for OX_1R and OX_2R, the *in vitro* competitive inhibition assays using OX_1R or OX_2R cells were carried out. The assay used Orexin A as the competitive ligand because of its affinity to OX_1R and OX_2R. The compounds synthesized showed higher binding affinities for OX_1R than OX_2R *in vitro*. Compounds **3** and **4** displayed superior binding affinities for OX_1R (at 30 and 31 nM, respectively) than OX_2R (160 and 332 nM, respectively). The selectivity for OX_1R (**3**) and OX_2R (**4**) were 5.3 and 10.6, indicating that THIQ derivatives selectively bind to OX_1R. A biodistribution study in normal mice was evaluated to determine the brain uptake of compounds **3** and **4**. The results showed that brain uptake of **3** was higher compared to **4,** and the radioactivity of compound **3** remained in the brain for 60 min. Thus, the brain-to-blood ratios of THIQ derivatives increased with time, but the maximum uptake (**3**: 0.99% ID g^{-1}, and **4**: 0.57% ID g^{-1}) and blood-to-brain ratio (**3**: 0.44, and **4**: 0.34) were not satisfactory for *in vivo* brain imaging. Although the compounds synthesized are potentially imaging probes for PET targeting the OX_1R, optimization or structural changes are needed to improve their brain uptake (Figure 3).

The importance of substitution in positions 6 and 7 of the THIQ moiety and the effect of removing one of the methoxy groups as a selective antagonist of OX_1R has been reported [19]. The activity of the targeted compounds **5**–**7** at

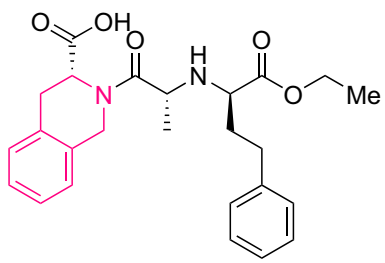

Quinapril
angiotensin-converting enzyme (ACE) inhibitor

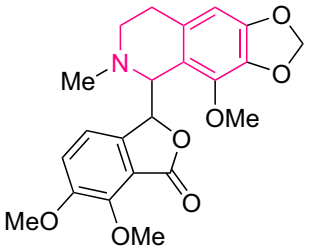

Noscapine
antitumor

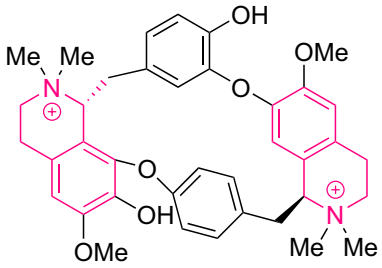

Tubocurarine
neuromuscular blocking agent

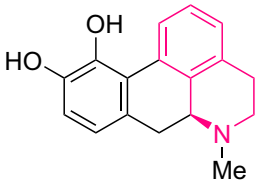

Apomorphine
non-selective dopamine agonist

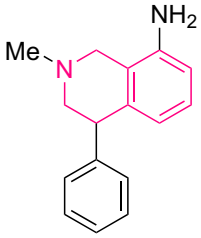

Nomifensine
norepinephrine-dopamine reuptake inhibitor

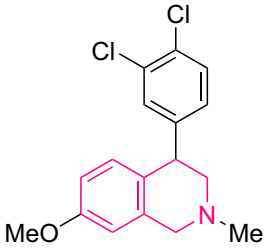

Diclofensine
triple monoamine reuptake inhibitor

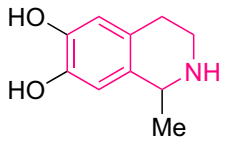

Salsolinol

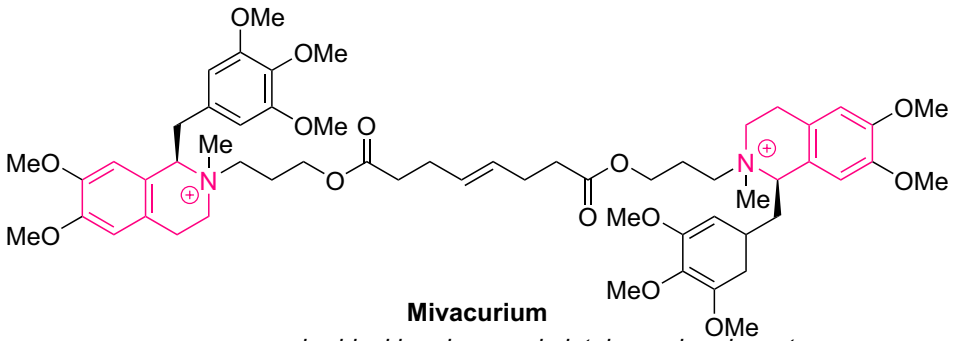

Mivacurium
neuromuscular-blocking drug or skeletal muscle relaxant

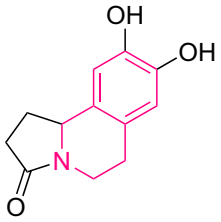

Oleracin E
antioxidant and antidepressant agent

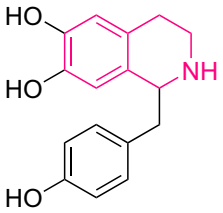

Higenamine
agonist for beta-2-adrenergic receptor, antimycobacterial, and anti-inflammatoric drug

Figure 1. Some naturally occurring and clinically available THIQ-based compounds

the OX_1 and OX_2 receptors was evaluated using calcium mobilization-based functional curve shift assays. The *n*-propyl derivative **5a** was the most potent compound of the series, with a *Ke* value of 23.7 nM, and was 108-fold greater selective for OX_1 over OX_2. The ethyl and isopropyl substituents showed slight potency compared to **5a**, (*Ke* = 37.3 nM and 49.7 nM, respectively), but had a superior OX_1 selectivity (268- and 201-fold, respectively). The position 7 is essential for the OX_1 antagonism. Meanwhile, several 6-amino compounds (**7**) containing ester groups showed a moderate potency (**7a**, *Ke* = 427 nM) (Figure 4).

Perrey et al. reported THIQ based compounds **8** and **9** with an excellent OX_1 potency and selectivity [20] (Figure 5). Most of the compounds synthesized demonstrated suitable activities. The introduction of a nitrogen atom into the structure did not significantly change the potency, but reduced the lipophilicity of these

ISSN 2308-8303 (Print) / 2518-1548 (Online)

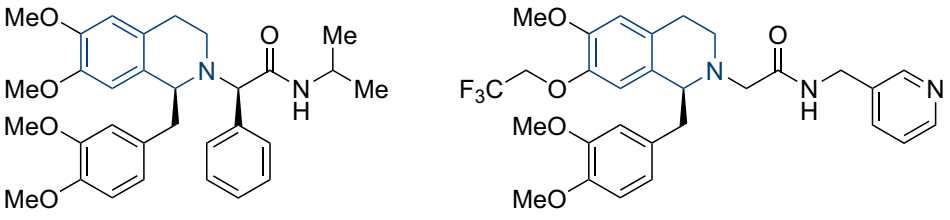

1

ACT-335827
OX_1 IC_{50} = 6 nM
OX_2 IC_{50} = 417 nM

2

RTIOX-276
OX_1 *Ke* = 8.5 nM
OX_2 *Ke* = 10,000 nM

Figure 2. Chemical structures of THIQ derivatives, ACT-335827 and RTIOX-276

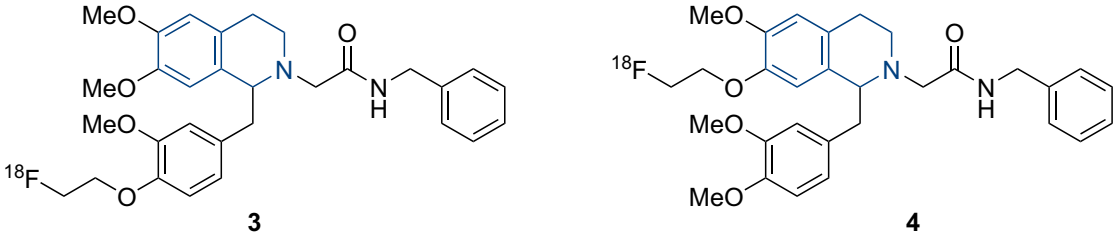

3

OX_1R IC_{50} = 30.3 ± 4.3 nM
OX_2R IC_{50} = 160.1 ± 38.5 nM

4

OX_1R IC_{50} = 31.3 ± 13.2 nM
OX_2R IC_{50} = 331.9 ± 82.0 nM

Figure 3. Chemical structures of THIQ derivatives acting as OX_1R antagonists

compounds. The 3-dimethylamino analog was the most potent in the first series, with a *Ke* value of 21 nM. When a pyridinylmethyl group was introduced in position 4, the potency was moderate (*Ke* = 96.4 nM), and the selectivity of > 100-fold. The substitution at the 1-benzyl position results in compounds with a good selectivity for the OX_1 receptor over the OX_2 receptor. Meanwhile, the replacement of benzylacetamide with the 3-pyridyl group displayed OX_1 antagonists (compound **9a**, *Ke* = 5.7 nM). The calculated clogP and PSA value of compound **9a** were 3.07 and 70, respectively, suggesting the solubility of compounds. Further study showed that **9a** displayed a good kinetic solubility (> 200 μM) and BBB permeability. Besides, compound **9a** possessed the low Pgp activity with an efflux ratio of 3.3.

PDE4 inhibitors

Phosphodiesterase is an enzyme with unique functions, hydrolyzing the cyclic nucleotides, such as cyclic adenosine-3,5-monophosphate (cAMP) and cyclic guanosine-3,5-monophosphate (cGMP), to their inactive 5′-nucleotide monophosphate, 5′-AMP and 5′-GMP, respectively [21, 22]. Phosphodiesterase 4 (PDE4) is a cAMP specific hydrolase and is identified as one of the 11 members of the PDE super-family. In addition, it predominates in many cells, such as keratinocytes, endothelial cells, hematopoietic cells, and nerve cells. PDE4 is encoded by four genes PDE4A, PDE4B, PDE4C, and PDE4D, with separate, distinct cellular distributions and functions. PDE4 plays a central role by regulating pro-inflammatory and anti-inflammatory cytokines and cell proliferation via the degradation of cAMP [23]. This has made PDE4 a leading target for the treatment of inflammatory diseases, such as psoriasis, arthritis, and atopic dermatitis. Three PDE4 inhibitors have been clinically evaluated and approved for treating inflammatory disease: roflumilast, apremilast, and crisaborole. To discover potent and effective PDE4B inhibitors, a 3-substituted carboxylic ester was incorporated into the THIQ scaffold **10–13** (Figure 6). All the targeted compounds were evaluated for their inhibitory activity *in vitro* against PDE4B, using rolipram as a positive control [24]. The IC_{50} values of the compounds being assessed displayed moderate to good inhibition against PDE4B between IC_{50} values of 0.95–23.25 μM. Compound **13a** showed the most potent inhibitory activity against PDE4B with an IC_{50} of 0.88 μM, which was 21-fold superior and with more potent selectivity toward PDE4B than PDE4D compared to rolipram. The structure-activity relationship study showed that the presence of either the electron-donating groups, such as the hydroxyl or methoxy group, or the electron-withdrawing group OCF_3 to the phenyl ring in the *para*-position improved the inhibitory activity against PDE4B.

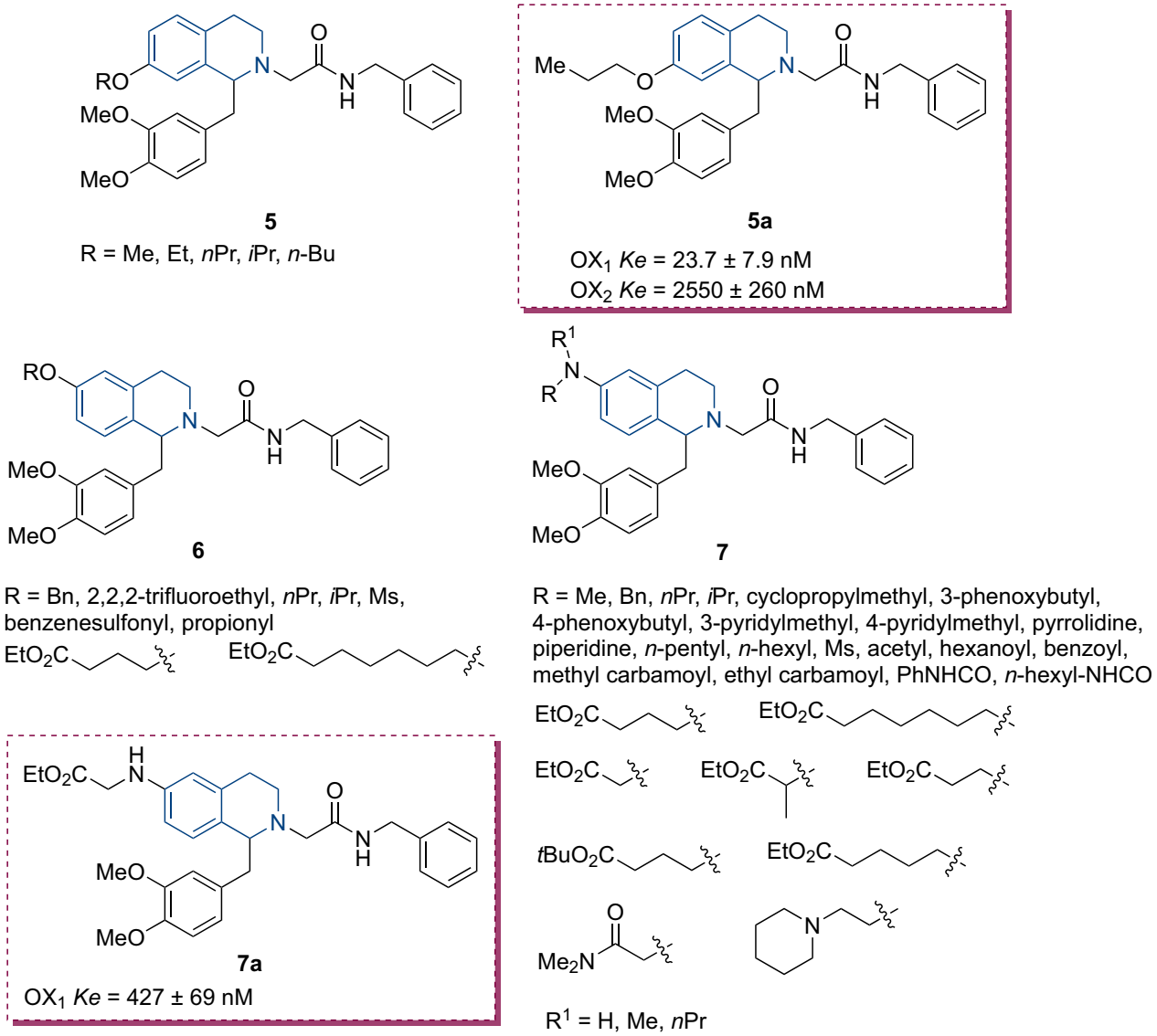

Figure 4. The chemical structure of THIQ derivatives acting as orexin receptor antagonists

The development, synthesis, and pharmacological evaluation of novel phosphodiesterase 4 (PDE4) inhibitors containing 7-(cyclopentyloxy)-6-methoxy-1,2,3,4-tetrahydroisoquinoline ring were reported **14–17** [25]. The compounds synthesized exhibited considerable effects on PDE4B. Among them, compound **14f** displayed a promising inhibitory effect with IC_{50} of 2.3 μM, which was comparable to the positive control – rolipram (IC_{50} = 1.3 μM) (Figure 7). The SAR studies showed that multiple substitution effects in the ring B (R^1, R^2 and R^3) demonstrated that the modification of the ring B was crucial. The presence of halogen atoms, such as F (**14b**, IC_{50} = 23.3 μM) and Cl (**14c**, IC_{50} = 15.5 μM), resulted in a superior or comparable activity in relation to the unsubstituted derivative (**14a**, IC_{50} = 23.5 μM).

Meanwhile, substituting methoxy groups in the *ortho* position of the phenyl ring B lessens the inhibitory activity against PDE4B (**14d**, IC_{50} = 37.0 μM). The substitution of methoxy and hydroxyl groups to the phenyl ring B in the *meta* and *para* positions gave the most active compound **14e**; this indicated that electron-donating groups in these positions favored the bioactivity. The activity decreased drastically when the benzene or pyridine ring was changed to cyclohexane (compounds **16** and **17**) (Figure 7). This may be due to the presence of three free hydroxyl groups and an amine hydrochloride on the cyclohexane ring, respectively. The docking study of the most active compound revealed that the catechol diether formed hydrogen bonds with the conserved Gln443, and the THIQ moiety was notably positioned between Phe446 and Ile410. The *para*-hydroxyl group of benzoyl imide formed a hydrogen bond with Asp27 and His234 to enhance the binding affinity with the enzyme.

ISSN 2308-8303 (Print) / 2518-1548 (Online)

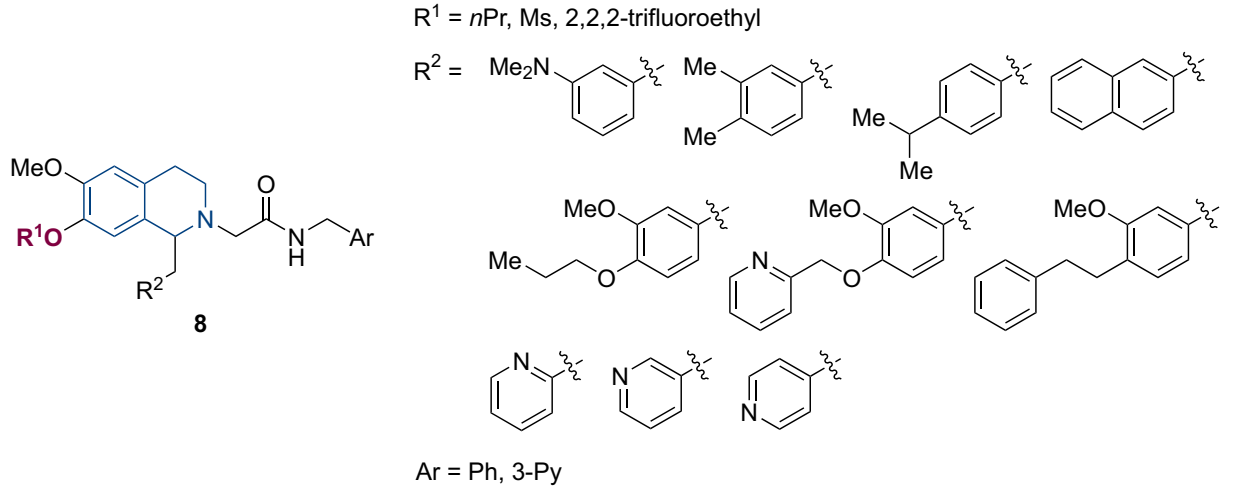

Figure 5. The chemical structure of a THIQ based compound that displayed promising orexin receptor antagonists

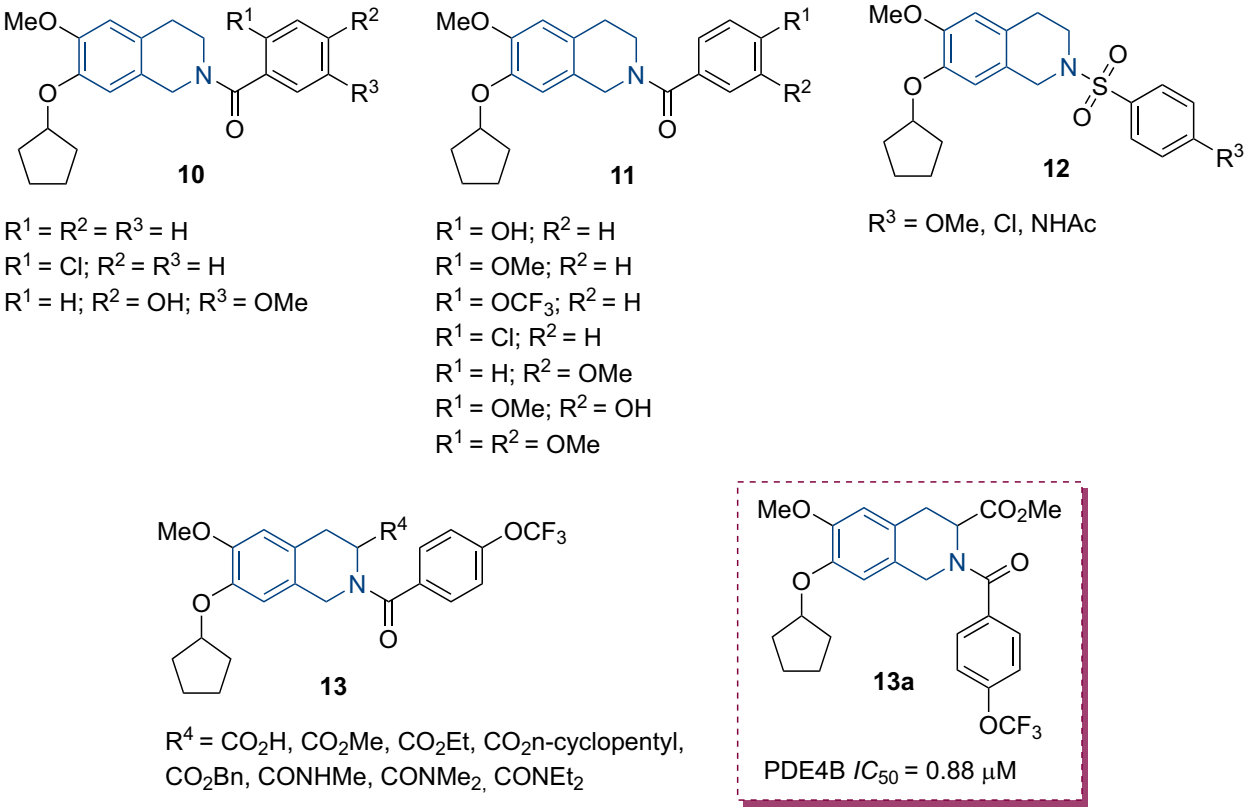

Figure 6. Chemical structures of compounds showing a promising inhibitory activity *in vitro* against PDE4B

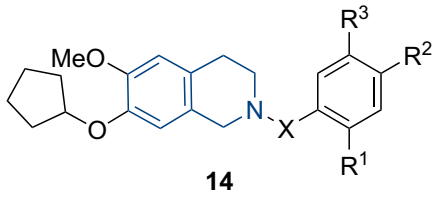

14

14a: X = CO, $R^1 = R^2 = R^3$ = H
14b: X = CO, R^1 = F, $R^2 = R^3$ = H
14c: X = CO, R^1 = Cl, $R^2 = R^3$ = H
14d: X = CO, R^1 = OMe, $R^2 = R^3$ = H
14e: X = CO, R^1 = H, R^2 = OH, R^3 = OMe
14f: X = CH_2, R^1 = F, $R^2 = R^3$ = H
14g: X = CH_2, R^1 = H, R^2 = O, R^3 = OMe

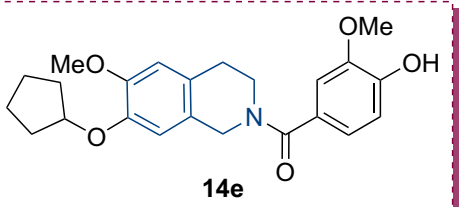

14e

PDE4B IC_{50} = 2.3 μM

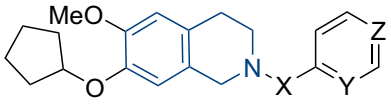

15

15a: X = CO, Y = N, Z = CH
15b: X = CO, Y = H, Z = N
15c: X = CH_2, Y = CH, Z = N

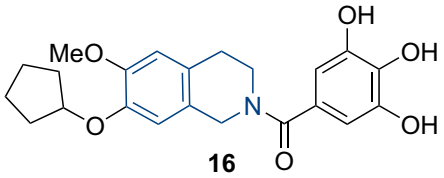

16

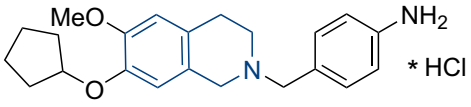

17

Figure 7. The chemical structure of compounds showing a promising inhibitory activity *in vitro* against PDE4B

SGLT2 inhibitors

Sodium-dependent glucose cotransporters (or sodium-glucose-linked transporter, SGLT) are a glucose transporter family. SGLT2 is responsible for more than 90% of the renal glucose reabsorption, whereas SGLT1 is for the remaining 10%. This indicated that renal glucose reabsorption is referred mainly by SGLT2 and to a reduced amount by SGLT1. Hence, selective SGLT2 inhibitors would be suitable for antidiabetic agents, and many SGLT2 inhibitors as antidiabetic agents have been approved [26, 27]. *Pan and coworkers* synthesized and evaluated a series of novel THIQ-based C-aryl glucosides to inhibit human SGLT2 [28] (Figure 8). The SGLT2 inhibitors were studied by substituting the proximal phenyl ring of dapagliflozin (**18**) with the conformation restricted THIQ ring (compounds **19** and **20**). All the compounds synthesized were evaluated in a cell-based SGLT2 functional assay in a concentration of 10 mM, and dapagliflozin was used as the reference compound. Compound **19a** containing a naphthalene ring exhibited great potency in the SGLT2 inhibitory activity (81.7%) compared to dapagliflozin (85.4%). The SAR studies showed that the introduction of thiophene resulted in the unfavored inhibitory activity against SGLT2, indicating that an electron-rich ring was not tolerant in this position. The introduction of the weakly electron-donating C_2H_5 group increased the inhibitory activity compared to the strong electron-donating (C_2H_5O group). The replacement of C_2H_5 with phenyl significantly increased the inhibitory activity. Since dapagliflozin and compound **19a** exhibited a comparable inhibitory activity *in vitro* against SGLT2, this might be a promising hit for treating type 2 diabetes.

P-glycoprotein inhibitors

P-glycoprotein (P-GP) can reduce absorption; it also has poor oral bioavailability, and can decrease the retention time of several drugs in coordination with the intestinal wall metabolism [29, 30]. It is noteworthy that P-GP is one of the leading barriers to cancer treatment with chemotherapy. A series of new P-GP inhibitors **21** (Figure 9) were designed and synthesized. The compounds were combined with doxorubicin in MCF-7/ADR cells to evaluate their reversal activity against multidrug resistance (MDR) [31].

ISSN 2308-8303 (Print) / 2518-1548 (Online)

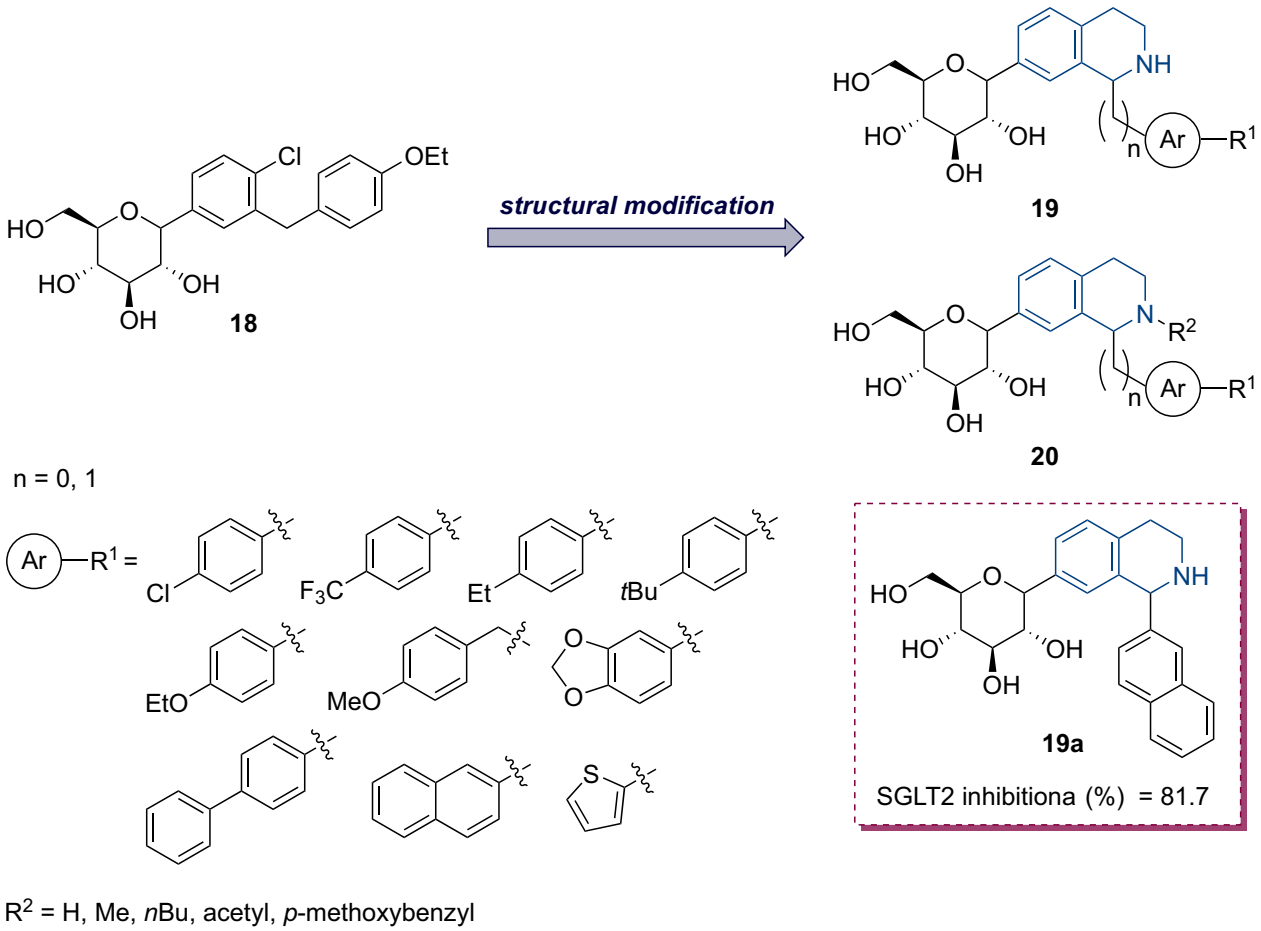

Figure 8. Compound **19a** containing a naphthalene ring exhibited great potency in the SGLT2 inhibitory activity

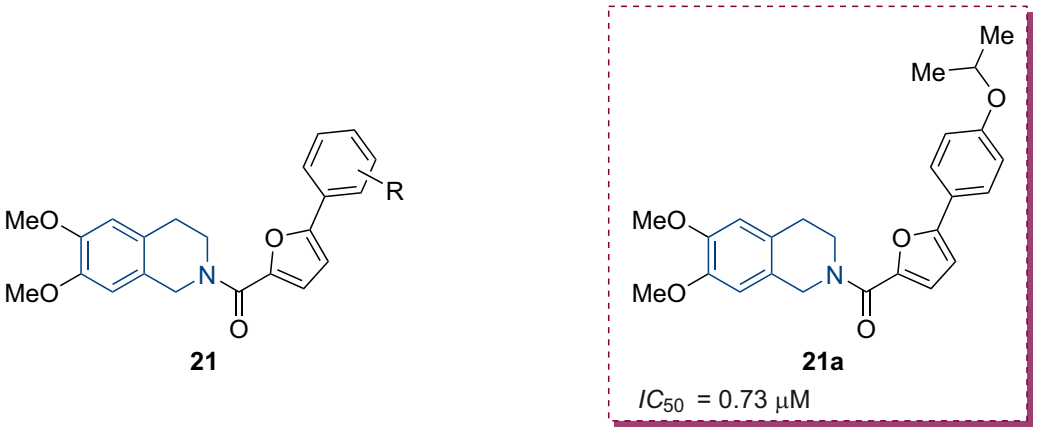

Figure 9. Compound **21a** containing isopropoxy displayed higher potency against P-GP

Compound **21a** containing the isopropoxy group displayed higher potency against P-GP mediated MDR in MCF-7/ADR (IC_{50} (doxorubicin) = 0.73 μM, RF = 69.6 with 5 μM **21a** treated). Further studies showed that **21a** efficiently inhibited the P-GP efflux function but not its expression. The reversal activity of compound **21a** at 5 μM against doxorubicin in MCF-7/ADR exceeded that of all compounds tested, including the positive controls – cyclosporin A (IC_{50} (DOX) = 0.86 μM, RF = 59.1) and verapamil (IC_{50} (DOX) = 4.25 μM, RF = 11.9). The SAR studies showed that the moderate activity was observed in the compound containing more than one methoxy group in the

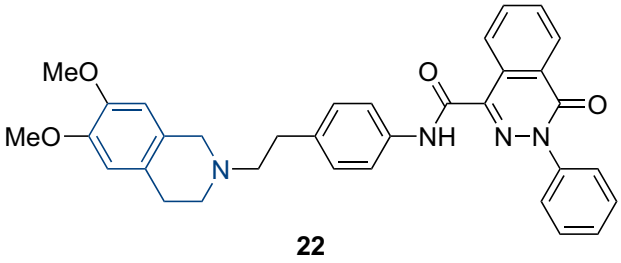

22

R = H, 3-Me, 4-Me, 2-Et, 3-MeO, 2-F, 3-F, 2-Br, 3-Br, 4-Cl, 4-NO_2, 4-CN, 3,4-*di*-Me, 2,5-*di*-F, 3,4-*di*-Cl, 3,5-CF_3, 2-Py

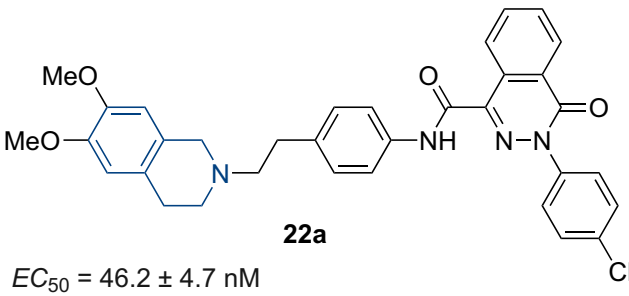

22a

EC_{50} = 46.2 ± 4.7 nM

Figure 10. Compound **22a** displayed a high promising inhibitory activity against doxorubicin resistant K562/A02 cells

benzene ring. Meanwhile, the length of the saturated aliphatic chain and the appropriate steric substituents, such as the isopropyl group, are essential to achieve the best activity. The molecular docking analysis demonstrated that compound **21a** formed a crucial hydrogen bonding interaction between the oxygen atom of the furan ring and the NH of Gln721. Besides, there was a lack of amino acid residues around the isopropoxy group that could generate intermolecular actions.

A series of novel P-GP-mediated MDR modulators containing phthalazinone and THIQ scaffolds were designed and synthesized by *Qiu et al.* [32]. Most of the targeted compounds **22** are superior to the standard (verapamil) (Figure 10). Among the targeted compounds, **22a** displayed a high promising inhibitory activity against doxorubicin-resistant K562/A02 cells with a low EC_{50} (46.2 ± 4.7 nM) and the lack of cytotoxicity towards normal cells (IC_{50} > 100 μM). The number and position of substituents on the ring significantly influence the reversal activity. Substitution in position 3 of the phenyl ring led to a steady or reduced activity, while substitution in position 4 gave a strong activity. In addition, an increase in the number of substituents reduces the activity. The molecular docking studies described in detail the interaction between the residues and compound **22a** in the hydrophobic pocket of the P-GP. Compound **22a** formed the H-bond interaction with the residue Gln 721 and the π-π stacking interaction with Tyr 303. The tertiary amine N atom of compound **22a** captures a hydrogen ion, developing a positive charge center to interact with the residue Phe728; this interaction helps to maintain the activity.

A new MDR reversal agent was designed and synthesized by selecting tariquidar as the lead compound and triazole as the bioisoster to replace benzene. The amido bond was modified by the secondary amine [33]. Thus, the click chemistry method linked the various chemical structures to the aromatic amides yielding compounds **23** and **24** (Figure 11). Among the compounds tested, compound **23a** containing the 3,4-dimethoxy group in the benzene ring demonstrated a potent effect compared to the positive control and the lack of cytotoxicity towards K562 and K562/ A02 cells. The MDR reversal effect of compound **23a** (IC_{50}/DOX (μM) = 1.30 ± 0.35, RF = 18.7) could last over a certain period, longer than that of VRP. Further research suggested that compound **23a** displayed a significant potency in an increased doxorubicin accumulation in K562/A02 cells and further decreased the P-GP-mediated efflux of Rh123. The compound possessing three substituted dimethoxy groups showed a good potency, while derivatives of compound **24** demonstrated an insignificant activity.

To identify ideal P-GP inhibitors reversing MDR in non-toxic concentrations, THIQ based compounds were designed [34] (Figure 12). The MTT (3-(4,5-dimethylthiazolyl-2)-2,5-diphenyltetrazolium bromide) assay was used to evaluate the cytotoxicity of the compounds synthesized against the human erythroleukemia K562 cells and the adriamycin (ADM)-resistant K562/A02 cells. The well-known classical P-GP inhibitor (verapamil) was used as the reference compound. Most target compounds displayed a low cytotoxicity and exhibited more active MDR reversal activity than verapamil. Compound **25a** demonstrated the strongest reversal activity with IC_{50} of 1.76 ± 0.3 μM. Further studies suggested that the most active compound effectively impeded the ADM efflux function of P-GP and augmented the accumulation of ADM in K562/A02 cells. Thus, **25a** is a promising candidate for developing P-GP-mediated MDR reversal modulator in cancer chemotherapy.

ISSN 2308-8303 (Print) / 2518-1548 (Online)

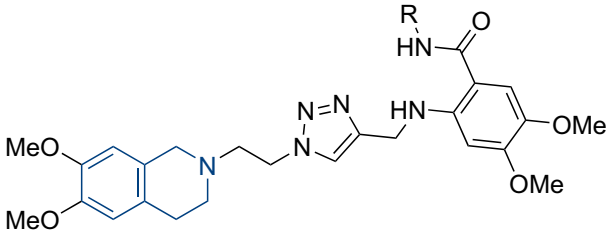

23

R = *i*Bu, Bn, Ph, 4-*t*Bu-Ph, 2-Me-Ph, 4-MeO-Ph, 2-MeO-Ph, 3,4,5-*tri*-MeO-Ph, 4-F-Ph, 4-Cl-Ph, 4-Br-Ph,

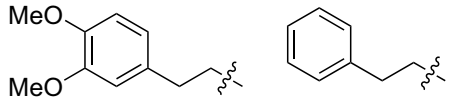

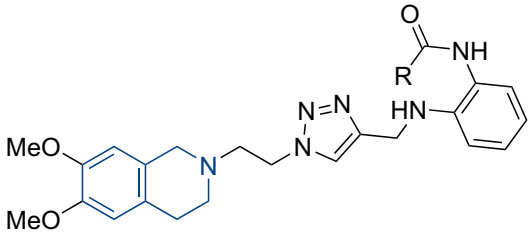

24

R = 2-NO_2-Ph, 3,4-*di*-NO_2-Ph, 2-Me-Ph, 2-Cl-Ph, 4-CN-Ph

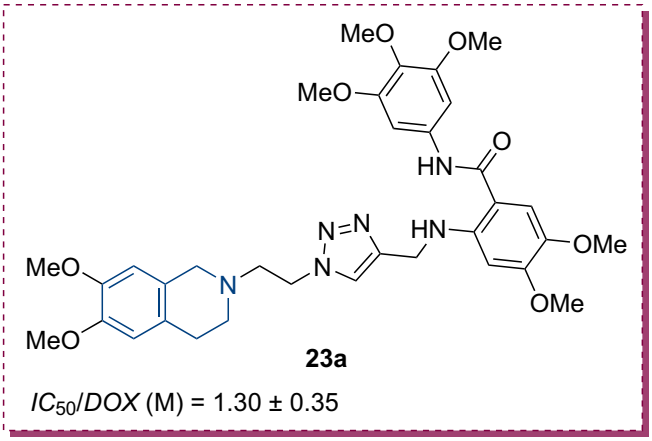

23a

IC_{50}/*DOX* (M) = 1.30 ± 0.35

Figure 11. The chemical structure of compound **23a** that displayed a significant potency in an increased accumulation of doxorubicin in K562/A02 cells

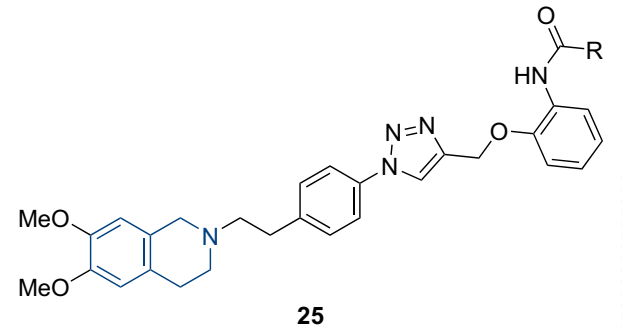

25

R =

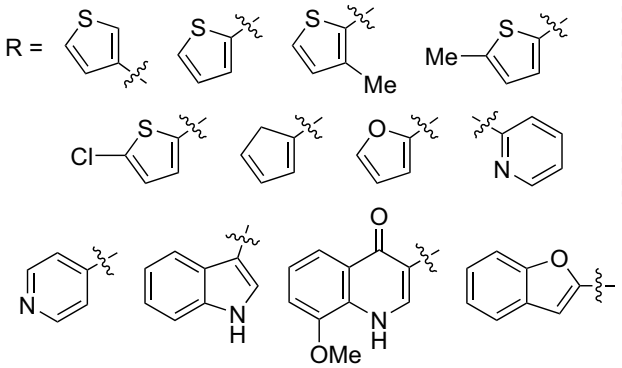

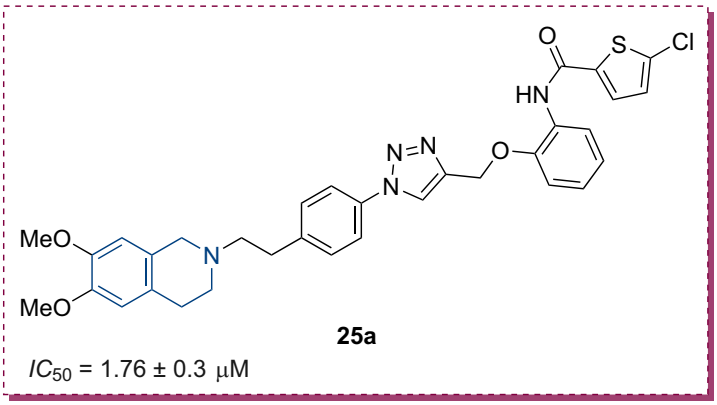

25a

IC_{50} = 1.76 ± 0.3 μM

Figure 12. The chemical structure of compound **25a** that demonstrated the strongest reversal activity

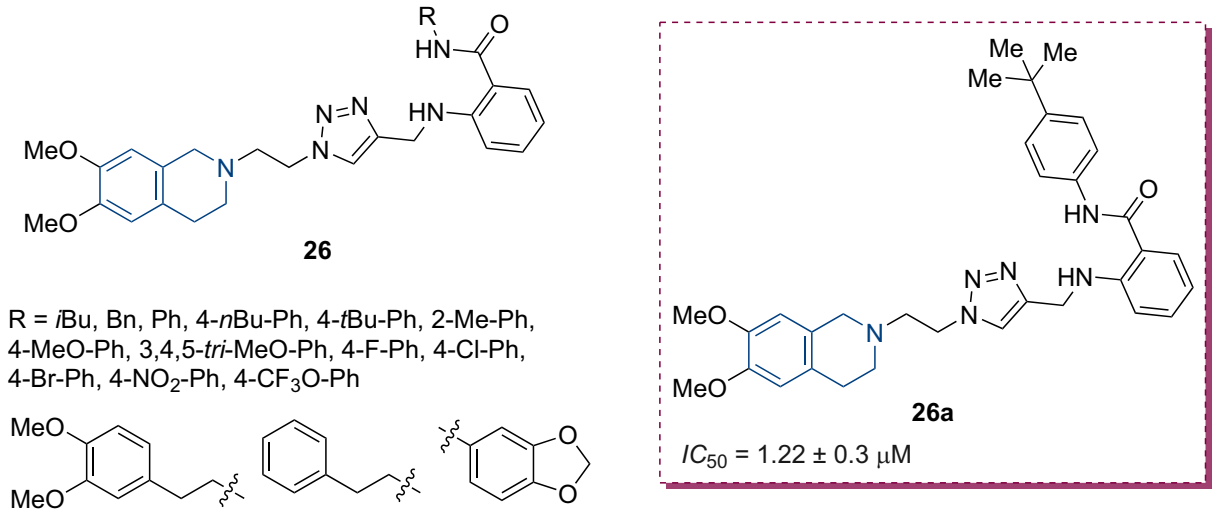

Figure 13. The chemical structure of a potent compound against P-GP

A total of 17 novel THIQ P-GP inhibitors were designed and synthesized by structure simplification and bioisosterism [35]. The results *of in vitro* cytotoxicity and reversed MDR activity showed that all the targeted compounds demonstrated no significant cytotoxicity with IC_{50} > 30 μM on both K562 and K562/A02 cells (P-GP overexpressed). Compound **26a** had the reversal activity, which was superior to the control (verapamil), significantly increased ADM accumulation in K562/A02 cells, and obstruct the efflux of Rh123 concurrently (Figure 13). The SAR studies showed that the compound with 4-*tert*-butylphenyl substituent displayed the highest activity (IC_{50} = 1.22 ± 0.3 μM), while the compound with 3,4-dimethoxyphenethyl substituent was somewhat inactive with IC_{50} of 41.48 ± 1.7 μM. In addition, the compounds containing substituents in position 4 of the benzene ring had a significant activity compared to those containing substituents in positions 3, 4. Compound **26a** interacted with the P-GP receptor *via* the π-π interaction of the aromatic ring and the hydrophobic interaction. The superimposition with tariquidar indicated that the target compound **26a** might have a similar binding site with the tariquidar in the active pocket of the P-GP receptor.

A library of P-GP inhibitors **28** was designed using alkyl as a linker between the phenolic group of the biphenyl moiety of compound **27** and various furazan derivatives containing substituents with different stereoelectronic and lipophilic properties [36] (Figure 14). Among the compounds tested, **28a–d** displayed the highest activity with EC_{50}, of 0.97 nM, 1.3 nM, 0.60 nM, and 0.90 nM, respectively, making them potential candidates for reverting MDR by co-administration of chemotherapeutic drugs and P-GP modulating agents. All the target compounds were inactive against MRP1 and BCRP transported. In addition, the high-affinity substrate profile of the active compounds (**28a–d**) is attractive because of their possible employment *in vivo* imaging of the function of P-GP through non-invasive imaging techniques, such as PET and SPECT.

A series of THIQ derivatives **29–31** containing the 5-phenyl-2-furan moiety were synthesized, and their P-GP potency and selectivity were evaluated [37] (Figure 15). Cyclosporin A and verapamil were adopted as the positive controls. Compound **31a** containing 6,7-dimethoxy and methoxyl groups in the *para*-position of the benzene ring showed the best bioactivity against P-GP (EC_{50} = 0.89 μM) among all the title compounds, which displayed better activity than both cyclosporin A and verapamil with an EC_{50} value of 83.68 μM and 20.54 μM against P-GP, respectively, compared to MC113 [38, 39]. Comparing the inhibitory activity of these three series, compound **29** containing the 6,7-dimethoxy group demonstrated a superior bioactivity than compounds **30** and **31**. Meanwhile, the presence of substituents in the *para*-position of the benzene ring suggested that the position was crucial for bioactivity. Compound **31a** with the highest inhibitory activity increased doxorubicin accumulation 9.2-fold at 20 μM in overexpressing P-GP MCF-7/ADR cells. **31a** was well fitted in the P-GP active site. The hydrogen bond interaction was observed between the O atom of the furan ring and the H at amine of Gln721 (distance: 2.59 Å). The hydrophobic effect was observed with three methoxy groups (-OMe) at the benzene ring and THIQ, which enhanced the binding affinity with the enzyme.

Wu and coworkers synthesized and biologically evaluated new series of THIQ as P-GP-mediated

ISSN 2308-8303 (Print) / 2518-1548 (Online)

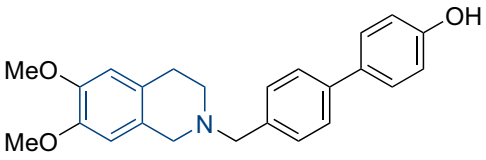

27

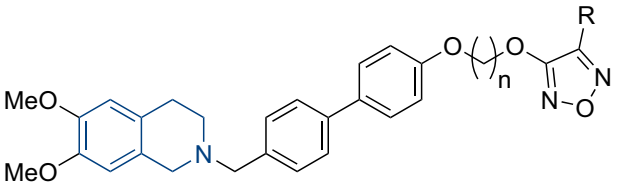

28

R = Ph, PhO, PhS, PhSO, $PhSO_2$, Me, MeO, $PhCH_2O$, CN
n = 2, 3, 4

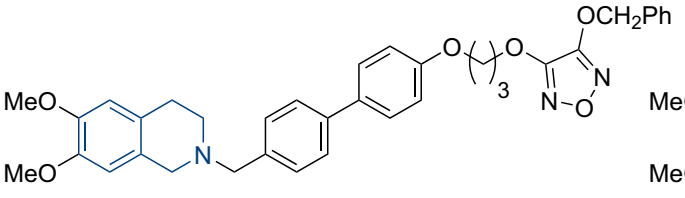

28a

EC_{50} = 0.97 nM

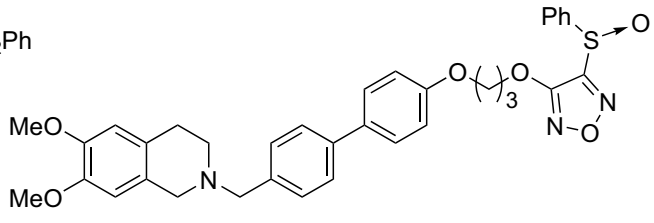

28b

EC_{50} = 1.3 nM

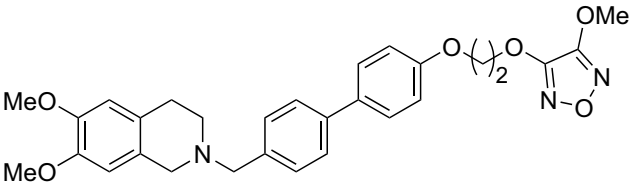

28c

EC_{50} = 0.60 nM

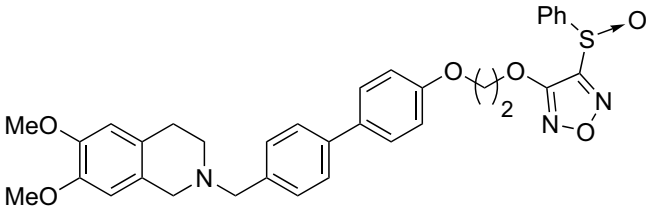

28d

EC_{50} = 0.90 nM

Figure 14. Chemical structures of potential candidates for reverting MDR

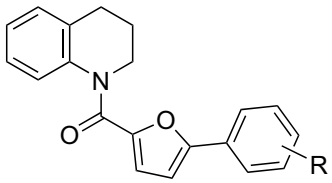

29

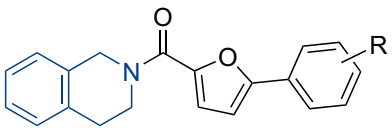

30

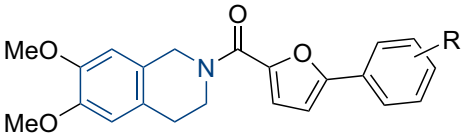

31

R = H, 2-Cl, 3-Cl, 4-Cl, 2-F, 3-F, 4-F, 2-NO_2, 3-NO_2, 4-NO_2, 4-Me, 4-Br, 4-MeO, 2,4-*di*-F, 2,6-*di*-F

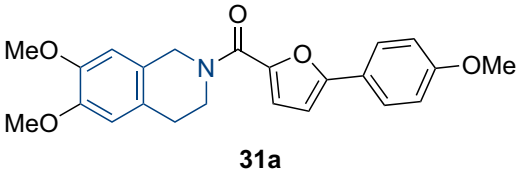

31a

EC_{50} = 0.89 μM

Figure 15. The chemical structure of a potent compound against P-GP

MDR inhibitors [40] (Figure 16). The effects of the target compounds on the reversing adriamycin (ADM) resistance toward K-562/A02 cells (P-GP-overexpression) were carried out using the MTT assay. The well-known classical P-GP inhibitor VRP, WK-X-34, and LBM-A5 were used as the positive control. Compounds with triazol-*N*-phenethyl-tetrahydroisoquinoline **32** were generally more potent than compounds with triazol-*N*-ethyl-tetrahydroisoquinoline **33**. Among them, compound **32a** with a pointedly decreased IC_{50} of ADM (1.21 ± 0.18 μM) showed the strongest reversal activity, and its reversal fold (RF) was 31.4 compared to WK-X-34 (RF = 30.4)

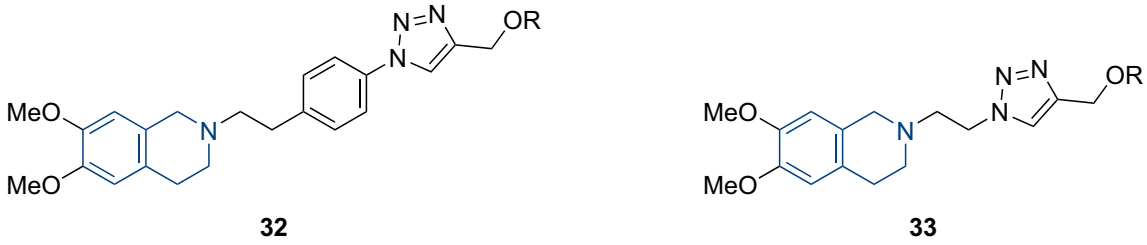

R = Ph, 2-NO_2-Ph, 4-NO_2-Ph, 4-Me-Ph, 4-*i*Pr-Ph, 4-*t*Bu-Ph, 2-*t*Bu-Ph, 3,4-*di*-Me-Ph, 2,4-*di*-Me-Ph, 4-F-Ph, 4-MeO-Ph, 2-MeO-Ph, 4-CF_3O-Ph, 1-naphthyl, 2-naphthyl,

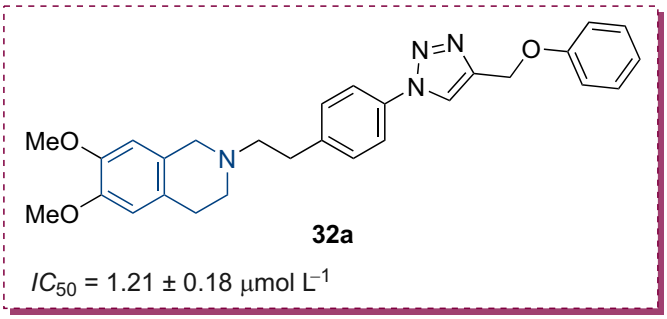

IC_{50} = 1.21 ± 0.18 μmol L^{-1}

Figure 16. The chemical structure of a promising compound that showed the best MDR reversal activity among twenty-five targeted compounds

and slightly higher than LBM-A5 (RF = 23.0). However, most of the targeted compounds exhibited more active MDR reversal activity than VRP when co-administered with ADM under the same condition. Electron-donating groups, such as $CH(CH_3)_2$ and $C(CH_3)_3$, showed higher MDR reversal activity than VRP, while OCH_3 showed lower MDR reversal activity than VRP. In addition, electron-withdrawing groups demonstrated a poor MDR reversal activity. The size of the substituent affects the MDR reversal activity. The compound containing 4-*tert*-butyl was more potent and showed more ADM accumulation in K562/A02 cells than the compound substituted by other alkyls. Compound **32a** and the compound with 4-*tert*-butyl substituent showed the best MDR reversal activity among the twenty-five target compounds, with IC_{50} of 1.21 ± 0.18 μmol L^{-1} and 1.86 ± 0.15 μmol L^{-1} compared to the lead compound LBM-A5 (IC_{50} = 1.65 ± 0.22 μmol L^{-1}).

Antibacterial

The synthesis of THIQ-triazole derivatives **34** and **35** was strategically designed by using the nitrogen atom of THIQ as an attachment to the terminal alkyne [41] (Figure 17). The alkyne allowed the incorporation of different substituted aromatic rings *via* the formation of the triazole ring using the Cu-catalyzed azide-alkyne cycloaddition. The compounds synthesized were evaluated against Gram-positive bacteria, namely *S. aureus* ATCC25923, *B. subtilis* 168, and *E. coli* MG1655. *S. aureus* ATCC25923 and methicillin. *B. subtilis* 168. Besides, non-pathogenic *E. coli* MG1655 was used as the model for Gram-negative organisms. All the compounds synthesized were initially screened for the growth inhibition activity against *S. aureus*. Most of the compounds gave a *MIC* value from 4 to 32 μg mL^{-1}, and compounds **34a–c** with *MIC* values of 4 μg mL^{-1} were observed as the promising candidates. Further research showed that all sixteen compounds were not active against Gram-negative *E. coli* in the concentration of 128 μg mL^{-1}. Compound **34a** with an unsubstituted aromatic ring showed no activity, indicating an increase in polarity or even the compound length/size may negatively impact the inhibitory properties. The introduction of the *tert*-butyl group increased the activity against *S. aureus* and *B. subtilis*. The introduction of hydrophobic groups, such as naphthalene and 4-biaryl, maintained the activity. The presence of hydrophilic and electron-withdrawing groups, namely 4-chloro, 4-cyano, 4-nitro, and 4-dimethyl carbamoyl groups, displayed no significant activity when tested against *S. aureus*. The presence of the CF_3 substituent, an electron-withdrawing group with hydrophobic properties, enhanced the action at the *MIC* of 32 μg mL^{-1} and 8 μg mL^{-1}, respectively. The introduction of a nucleophilic N-atom in 3,5-dichloropyridyl drastically reduced the inhibitory activity. It is noteworthy that the presence of electron-donating and electron-withdrawing effects merged with the hydrophobicity of either *tert*-butyl or OBn increased the activity of **34a–c**. In addition, compound **34a,** which effectively

ISSN 2308-8303 (Print) / 2518-1548 (Online)

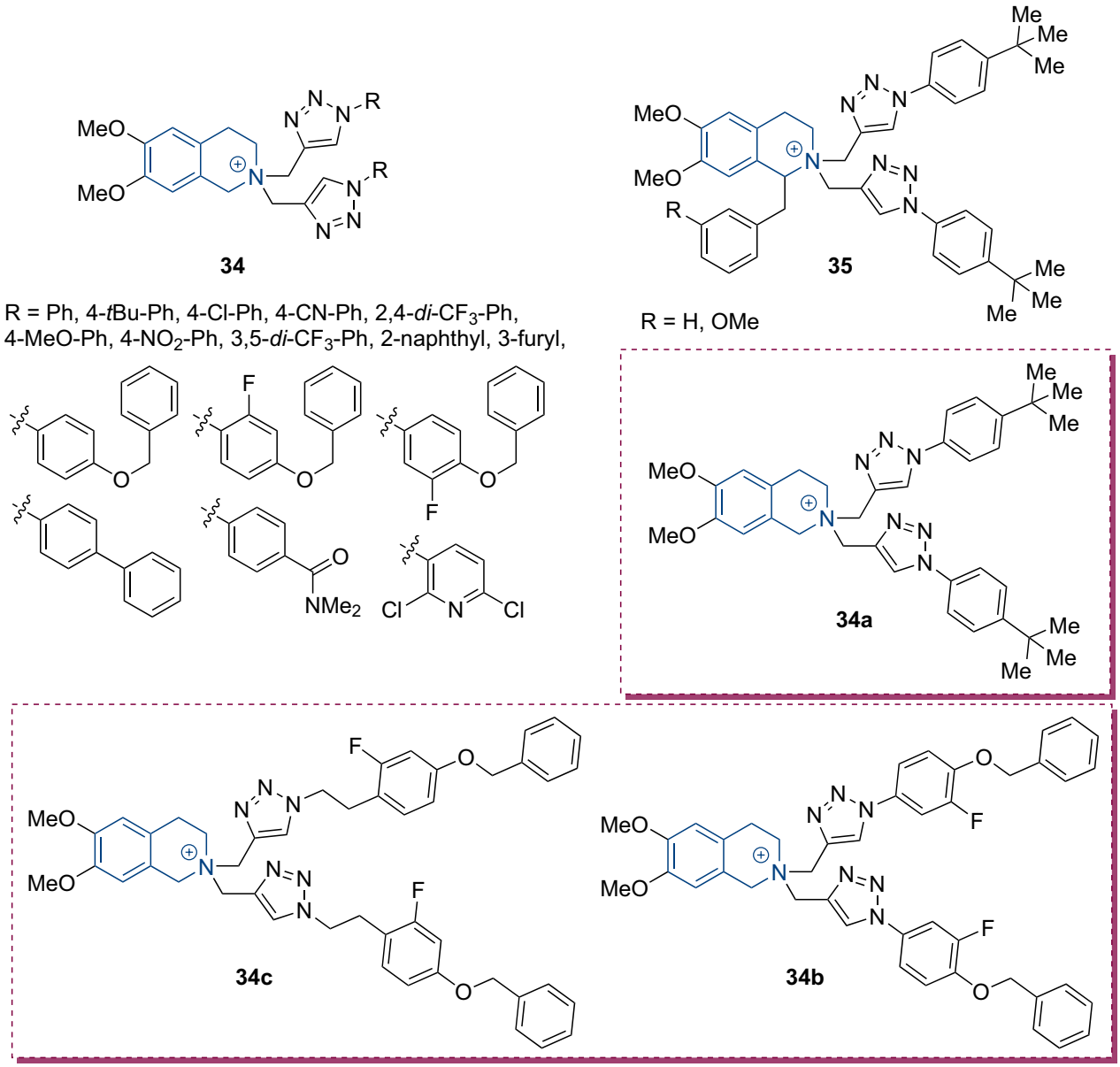

Figure 17. Chemical structures of promising THIQ compounds

inhibited *S. aureus*, prevented *M. tuberculosis* H37Rv at *MIC* of 6 μg mL^{-1} with the lack of resistance after thirty days of sequential passaging. These results identified compound **34a** and its analogs as potential candidates for further drug development for antibiotic resistance.

Anticancer

A series of fifteen THIQ derivatives **36**–**40** were synthesized, and their antiproliferative activity were reported [42] (Figure 18). All the compounds newly synthesized were screened for their anticancer activity against a panel of five human cancer cell lines, such as MCF-7 (breast cancer), DU-145 (prostate cancer), A549 (lung cancer), Hela (cervical cancer, and HepG2 (liver cancer) using the MTT assay. Most compounds showed a promising activity with IC_{50} values ranging from 0.72 to 92.6 μM. Among them, compounds **39a** and **39b** exhibited a significant activity against the prostate cancer cell line, namely DU-145, with IC_{50} values of 0.72 and 1.23 μM, respectively. The tubulin polymerization assay and the immunofluorescence determination suggested that these derivatives effectively prevented the microtubule assembly formation in DU-145. The results from further research, such as the cell cycle analysis, western blot, DNA-fragmentation analysis, caspase-3 activation studies, and annexin V-FITC assay of **39a** and **39b**, showed that the active compounds inhibited induced cell death by apoptosis.

New THIQ derivatives **41**–**44** were designed, synthesized, and biologically evaluated [43] (Figure 19). The KRas activity of five compounds tested (**42a**–**e**) was carried out on four different colon cancer cell lines (HCT KRasSL, RKO KRasSL,

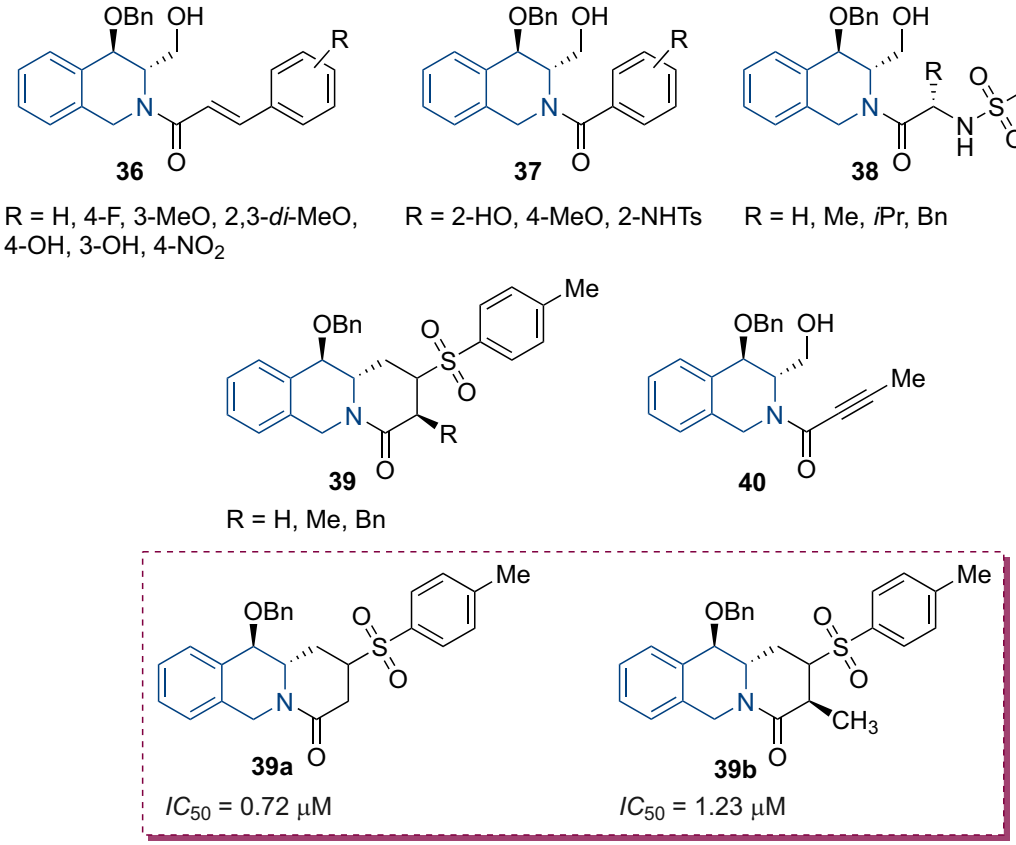

Figure 18. Chemical structures of compounds that exhibited a significant activity against the prostate cancer cell line

Colo 320 KRasSL, and SNU-C1 KRasSL) using three different concentrations (0.2 μM, 2 μM and 20 μM). The results showed that all the compounds studied had a higher overall KRas inhibition. Surprisingly, alcohol **42a** displayed a lower KRas inhibition than other analogs. The amine-containing compound **42c** demonstrated the highest KRas activity profile on RKO KRasSL, revealing that a terminal ionic interaction led to an increased KRas inhibition. The N-aryl-containing compounds (**42d** and **42e**) had the highest KRas inhibition on the colon 320 KRas SL cell line, suggesting that a low electron density aromatic side chain structure resulted in higher KRas activity. Compound **42e** displayed a significant KRas activity in the concentration of 0.2 μM (RKO KRasSL 95.8% inhibition, HCT KRasSL 35.9% inhibition). In addition, amine **42c** and the alcohol **42a** derivatives exhibited a promising antileukemic activity (IC_{50} = 2.0 and 2.6 μM, respectively), and the study of cytotoxic mechanisms suggested the involvement of KRas inhibition in both without additional antiangiogenic effects in the case of compound **42a**. The antiangiogenic evaluation was carried out for **42a–e**. The results showed that **42b** and **42c** possessed an interesting antiangiogenic activity, while **42d** and **42e** exhibited an insignificant activity, and **42a** was inactive. Compound **42b** containing the nitrile group was the most potent antiangiogenic agent. It displayed the highest antiangiogenic (IC_{50} = 2.9 μM) and anti-osteoporotic activity, indicating that the dipolar lipophilic terminal group, such as the nitrile group, enhanced the antiangiogenic and anti-osteoporotic activity.

To identify promising anticancer agents, a new series of THIQ derivatives **45** and **46** were designed and synthesized [44] (Figure 20). The targeted compounds were tested against different human cancer cells. Compounds **45**, incorporating either hydroxyl or trifluoromethyl groups in the R^3 position of the phenyl ring displayed a moderate antiproliferative activity with the GI_{50} value of 4.365 and 4.224 μM, respectively, whereas the incorporation of the methoxy group in the same position led to the loss of activity. For the THIQ scaffold containing a 4-chlorobenzoyl group, the derivatives with methoxy groups exhibited a significant activity on gastric cancer cells, whereas all three compounds with hydroxyl substituents had an inferior activity. Compound **46a** with an *ortho*-methoxy group led to a 2-fold higher activity (GI_{50} value = 1.591 μM) than the compound containing a *para*-methoxy group (GI_{50} = 3.627 μM).

ISSN 2308-8303 (Print) / 2518-1548 (Online)

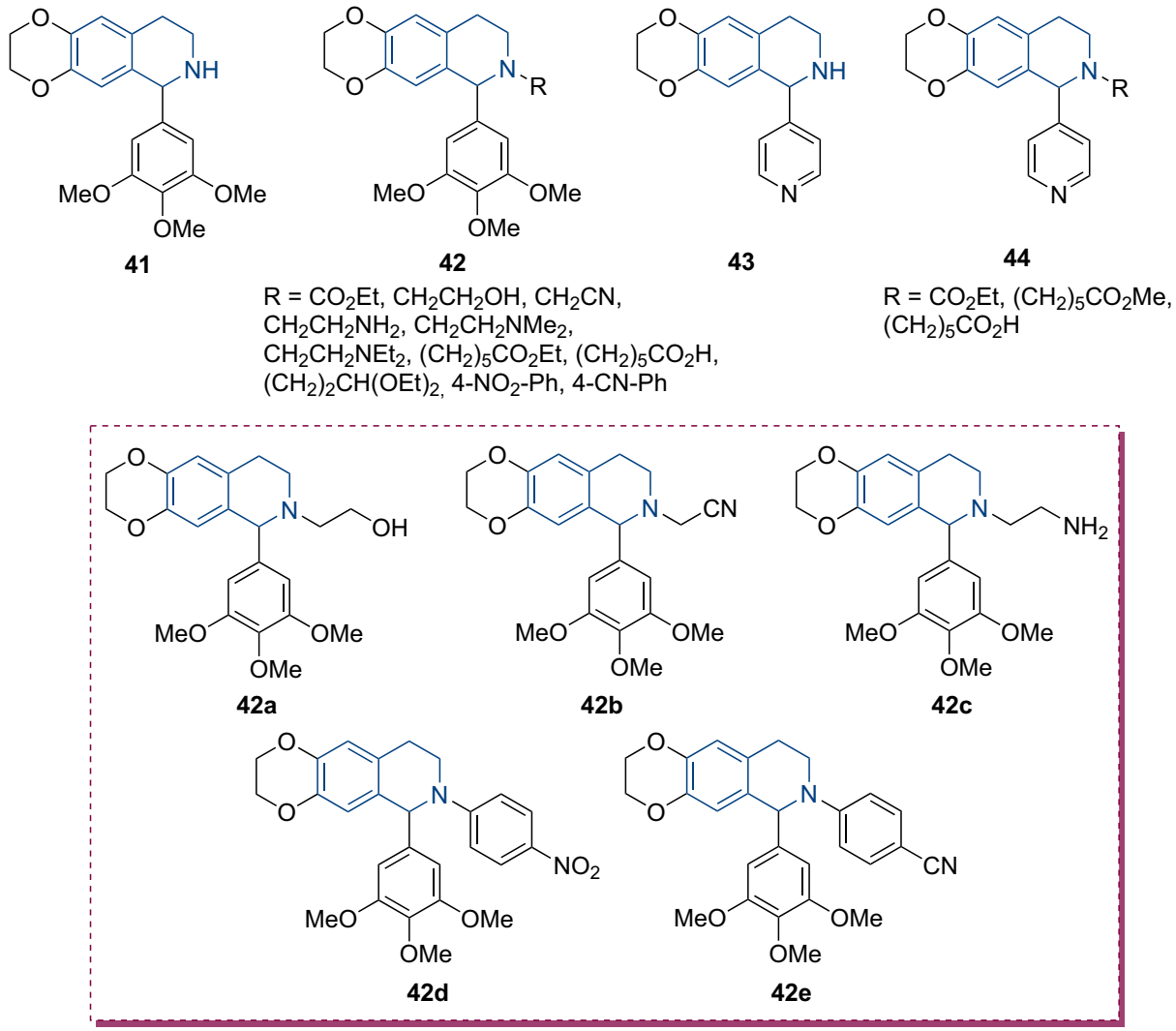

Figure 19. Chemical structures of promising anticancer agents containing the THIQ moiety

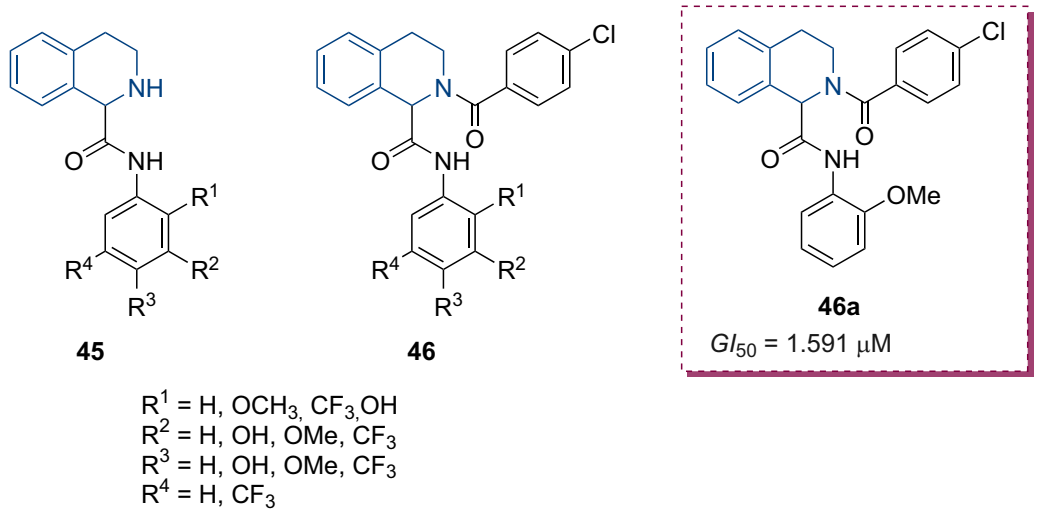

Figure 20. 1-Carbamoyl THIQ derivatives with a promising inhibitory activity against gastric cancer cells

CXCR4 antagonists

CXCR4 antagonists **47** with an increased liver microsomal stability in human and mouse models compared to the parent molecule TIQ-15 were reported [45] (Figure 21). Compounds **47a,b** containing chloro substituent on the pyridylmethyl moiety are the most promising candidates.

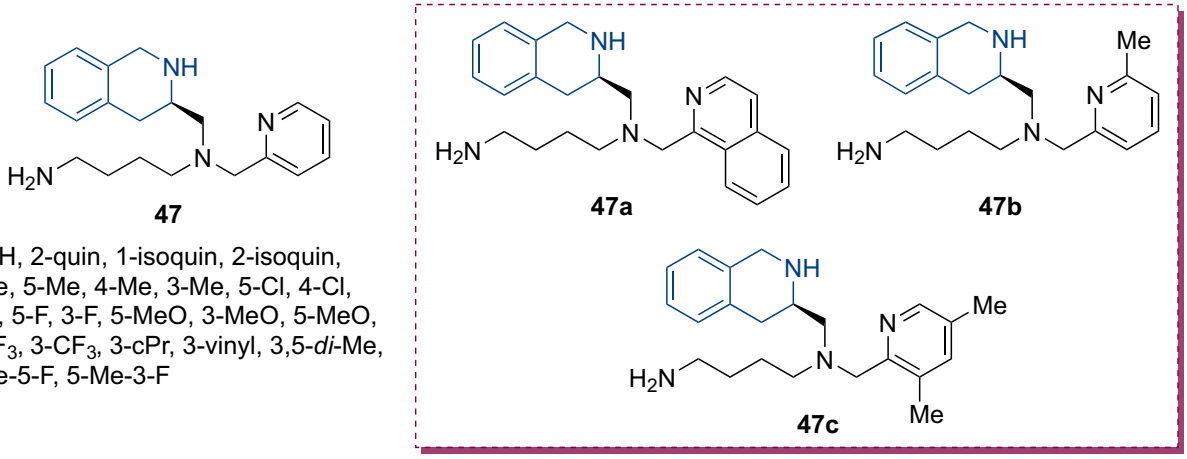

Figure 21. Promising CXCR4 antagonists with a THIQ backbone

■ Conclusions

This review presents a broad range of biological activities of THIQ, it will give the reader an idea of the therapeutic use of THIQ in various diseases. Due to the promising effect of THIQ in many biological activities, much attention has been paid to its therapeutic role. The SAR studies of the above-mentioned compounds show a better perception of the choice of an appropriate substitution model comprising electron-donating, electron-withdrawing and some heterocyclic functional groups on the backbone plays a vital role in modulating the biological potential of the compounds synthesized. This review will help pharmaceutical researchers to synthesize novel and potent compounds containing THIQ scaffold.

■ References

1. Wen, J.; Tan, R.; Liu, S.; Zhao, Q.; Zhang, X. Strong Brønsted acid promoted asymmetric hydrogenation of isoquinolines and quinolines catalyzed by a Rh-thiourea chiral phosphine complex via anion binding. *Chem. Sci.* **2016,** *7* (5), 3047–3051. https://doi.org/10.1039/c5sc04712a.
2. Bringmann, G.; Brun, R.; Kaiser, M.; Neumann, S. Synthesis and antiprotozoal activities of simplified analogs of naphthylisoquinoline alkaloids. *Eur. J. Med. Chem.* **2008,** *43* (1), 32–42. https://doi.org/10.1016/j.ejmech.2007.03.003.
3. Fayez, S.; Feineis, D.; Ake Assi, L.; Kaiser, M.; Brun, R.; Awale, S.; Bringmann, G. Ancistrobrevines E-J and related naphthylisoquinoline alkaloids from the West African liana Ancistrocladus abbreviatus with inhibitory activities against Plasmodium falciparum and PANC-1 human pancreatic cancer cells. *Fitoterapia* **2018,** *131*, 245–259. https://doi.org/10.1016/j.fitote.2018.11.006.
4. Kumar, A.; Katiyar, S. B.; Gupta, S.; Chauhan, P. M. Syntheses of new substituted triazino tetrahydroisoquinolines and beta-carbolines as novel antileishmanial agents. *Eur. J. Med. Chem.* **2006,** *41* (1), 106–113. https://doi.org/10.1016/j.ejmech.2005.09.007.
5. Lu, G. L.; Tong, A. S. T.; Conole, D.; Sutherland, H. S.; Choi, P. J.; Franzblau, S. G.; Upton, A. M.; Lotlikar, M. U.; Cooper, C. B.; Denny, W. A.; Palmer, B. D. Synthesis and structure-activity relationships for tetrahydroisoquinoline-based inhibitors of Mycobacterium tuberculosis. *Bioorg. Med. Chem.* **2020,** *28* (22), 115784. https://doi.org/10.1016/j.bmc.2020.115784.
6. Gabet, B.; Kuo, P. C.; Fuentes, S.; Patel, Y.; Adow, A.; Alsakka, M.; Avila, P.; Beam, T.; Yen, J. H.; Brown, D. A. Identification of N-benzyltetrahydroisoquinolines as novel anti-neuroinflammatory agents. *Bioorg. Med. Chem.* **2018,** *26* (21), 5711–5717. https://doi.org/10.1016/j.bmc.2018.10.020.
7. George, A.; Gopi Krishna Reddy, A.; Satyanarayana, G.; Raghavendra, N. K. 1,2,3,4-Tetrahydroisoquinolines as inhibitors of HIV-1 integrase and human LEDGF/p75 interaction. *Chem. Biol. Drug. Des.* **2018,** *91* (6), 1133–1140. https://doi.org/10.1111/cbdd.13175.
8. Chander, S.; Ashok, P.; Singh, A.; Murugesan, S. De-novo design, synthesis and evaluation of novel 6,7-dimethoxy-1,2,3,4-tetrahydroisoquinoline derivatives as HIV-1 reverse transcriptase inhibitors. *Chem. Cent. J.* **2015,** *9*, 33. https://doi.org/10.1186/s13065-015-0111-6.
9. Gitto, R.; Francica, E.; De Sarro, G.; Scicchitano, F.; Chimirri, A. Solution-phase parallel synthesis of novel 1,2,3,4-tetrahydroisoquinoline-1-ones as anticonvulsant agents. *Chem. Pharm. Bull. (Tokyo)* **2008,** *56* (2), 181–184. https://doi.org/10.1248/cpb.56.181.
10. Singh, K.; Pal, R.; Khan, S. A.; Kumar, B.; Akhtar, M. J. Insights into the structure activity relationship of nitrogen-containing heterocyclics for the development of antidepressant compounds: An updated review. *Journal of Molecular Structure* **2021,** *1237*, 130369. https://doi.org/10.1016/j.molstruc.2021.130369.
11. Kang, S. H.; Bak, D. H.; Yeoup Chung, B.; Bai, H. W. Transformation of nomifensine using ionizing radiation and exploration of its anticancer effects in MCF-7 cells. *Exp. Ther. Med.* **2022,** *23* (4), 306. https://doi.org/10.3892/etm.2022.11235.
12. Luethi, D.; Hoener, M. C.; Liechti, M. E. Effects of the new psychoactive substances diclofensine, diphenidine, and methoxphenidine on monoaminergic systems. *Eur. J. Pharmacol.* **2018,** *819*, 242–247. https://doi.org/10.1016/j.ejphar.2017.12.012.
13. Inutsuka, A.; Yamanaka, A. The physiological role of orexin/hypocretin neurons in the regulation of sleep/wakefulness and neuroendocrine functions. *Front. Endocrinol. (Lausanne)* **2013,** *4*, 18. https://doi.org/10.3389/fendo.2013.00018.
14. Tsujino, N.; Sakurai, T. Role of orexin in modulating arousal, feeding, and motivation. *Front. Behav. Neurosci.* **2013,** *7*, 28. https://doi.org/10.3389/fnbeh.2013.00028.
15. Steiner, M. A.; Gatfield, J.; Brisbare-Roch, C.; Dietrich, H.; Treiber, A.; Jenck, F.; Boss, C. Discovery and characterization of ACT-335827, an orally available, brain penetrant orexin receptor type 1 selective antagonist. *ChemMedChem* **2013,** *8* (6), 898–903. https://doi.org/10.1002/cmdc.201300003.

ISSN 2308-8303 (Print) / 2518-1548 (Online)

16. Perrey, D. A.; German, N. A.; Gilmour, B. P.; Li, J. X.; Harris, D. L.; Thomas, B. F.; Zhang, Y. Substituted tetrahydroisoquinolines as selective antagonists for the orexin 1 receptor. *J. Med. Chem.* **2013,** *56* (17), 6901–6916. https://doi.org/10.1021/jm400720h.
17. Perrey, D. A.; German, N. A.; Decker, A. M.; Thorn, D.; Li, J. X.; Gilmour, B. P.; Thomas, B. F.; Harris, D. L.; Runyon, S. P.; Zhang, Y. Effect of 1-substitution on tetrahydroisoquinolines as selective antagonists for the orexin-1 receptor. *ACS Chem. Neurosci.* **2015,** *6* (4), 599–614. https://doi.org/10.1021/cn500330v.
18. Watanabe, H.; Fukui, K.; Shimizu, Y.; Idoko, Y.; Nakamoto, Y.; Togashi, K.; Saji, H.; Ono, M. Synthesis and biological evaluation of F-18 labeled tetrahydroisoquinoline derivatives targeting orexin 1 receptor. *Bioorg. Med. Chem. Lett.* **2019,** *29* (13), 1620–1623. https://doi.org/10.1016/j.bmcl.2019.04.044.
19. Perrey, D. A.; Decker, A. M.; Li, J. X.; Gilmour, B. P.; Thomas, B. F.; Harris, D. L.; Runyon, S. P.; Zhang, Y. The importance of the 6- and 7-positions of tetrahydroisoquinolines as selective antagonists for the orexin 1 receptor. *Bioorg. Med. Chem.* **2015,** *23* (17), 5709–5724. https://doi.org/10.1016/j.bmc.2015.07.013.
20. Perrey, D. A.; Decker, A. M.; Zhang, Y. Synthesis and Evaluation of Orexin-1 Receptor Antagonists with Improved Solubility and CNS Permeability. *ACS Chem. Neurosci.* **2018,** *9* (3), 587–602. https://doi.org/10.1021/acschemneuro.7b00402.
21. Boswell-Smith, V.; Spina, D. PDE4 inhibitors as potential therapeutic agents in the treatment of COPD-focus on roflumilast. *Int. J. Chron. Obstruct. Pulmon. Dis.* **2007,** *2* (2), 121–129.
22. Essayan, D. M. Cyclic nucleotide phosphodiesterases. *J. Allergy Clin. Immunol.* **2001,** *108* (5), 671–680. https://doi.org/10.1067/mai.2001.119555.
23. Li, H.; Zuo, J.; Tang, W. Phosphodiesterase-4 Inhibitors for the Treatment of Inflammatory Diseases. *Front. Pharmacol.* **2018,** *9*, 1048. https://doi.org/10.3389/fphar.2018.01048.
24. Liao, Y.; Guo, Y.; Li, S.; Wang, L.; Tang, Y.; Li, T.; Chen, W.; Zhong, G.; Song, G. Structure-based design and structure-activity relationships of 1,2,3,4-tetrahydroisoquinoline derivatives as potential PDE4 inhibitors. *Bioorg. Med. Chem. Lett.* **2018,** *28* (7), 1188–1193. https://doi.org/10.1016/j.bmcl.2018.02.056.
25. Song, G.; Zhao, D.; Hu, D.; Li, Y.; Jin, H.; Cui, Z. Design, synthesis and biological evaluation of novel tetrahydroisoquinoline derivatives as potential PDE4 inhibitors. *Bioorg. Med. Chem. Lett.* **2015,** *25* (20), 4610–4614. https://doi.org/10.1016/j.bmcl.2015.08.043.
26. Nomura, S.; Sakamaki, S.; Hongu, M.; Kawanishi, E.; Koga, Y.; Sakamoto, T.; Yamamoto, Y.; Ueta, K.; Kimata, H.; Nakayama, K.; Tsuda-Tsukimoto, M. Discovery of canagliflozin, a novel C-glucoside with thiophene ring, as sodium-dependent glucose cotransporter 2 inhibitor for the treatment of type 2 diabetes mellitus. *J. Med. Chem.* **2010,** *53* (17), 6355–6360. https://doi.org/10.1021/jm100332n.
27. Nauck, M. A. Update on developments with SGLT2 inhibitors in the management of type 2 diabetes. *Drug Des. Devel. Ther.* **2014,** *8*, 1335–1380. https://doi.org/10.2147/DDDT.S50773.
28. Pan, X.; Huan, Y.; Shen, Z.; Liu, Z. Synthesis and biological evaluation of novel tetrahydroisoquinoline-C-aryl glucosides as SGLT2 inhibitors for the treatment of type 2 diabetes. *Eur. J. Med. Chem.* **2016,** *114*, 89–100. https://doi.org/10.1016/j.ejmech.2016.02.053.
29. Amin, M. L. P-glycoprotein Inhibition for Optimal Drug Delivery. *Drug Target Insights* **2013,** *7*, 27–34. https://doi.org/10.4137/DTI.S12519.
30. Varma, M. V.; Ashokraj, Y.; Dey, C. S.; Panchagnula, R. P-glycoprotein inhibitors and their screening: a perspective from bioavailability enhancement. *Pharmacol. Res.* **2003,** *48* (4), 347–359. https://doi.org/10.1016/s1043-6618(03)00158-0.
31. Li, Y. S.; Yang, X.; Zhao, D. S.; Cai, Y.; Huang, Z.; Wu, R.; Wang, S. J.; Liu, G. J.; Wang, J.; Bao, X. Z.; Ye, X. Y.; Wei, B.; Cui, Z. N.; Wang, H. Design, synthesis and bioactivity study on 5-phenylfuran derivatives as potent reversal agents against P-glycoprotein-mediated multidrug resistance in MCF-7/ADR cell. *Eur. J. Med. Chem.* **2021,** *216*, 113336. https://doi.org/10.1016/j.ejmech.2021.113336.
32. Qiu, Q.; Zhou, J.; Shi, W.; Kairuki, M.; Huang, W.; Qian, H. Design, synthesis and biological evaluation of N-(4-(2-(6,7-dimethoxy-3,4-dihydroisoquinolin-2(1*H*)-yl)ethyl)phenyl)-4-oxo-3,4-dihydrophthalazine-1-carboxamide derivatives as novel P-glycoprotein inhibitors reversing multidrug resistance. *Bioorg. Chem.* **2019,** *86*, 166–175. https://doi.org/10.1016/j.bioorg.2019.01.039.
33. Qiu, Q.; Shi, W.; Zhao, S.; Zhu, Y.; Ding, Z.; Zhou, S.; Kairuki, M.; Huang, W.; Qian, H. Discovery to solve multidrug resistance: Design, synthesis, and biological evaluation of novel agents. *Arch. Pharm. (Weinheim)* **2019,** *352* (10), e1900127. https://doi.org/10.1002/ardp.201900127.
34. Zhang, B.; Zhao, T.; Zhou, J.; Qiu, Q.; Dai, Y.; Pan, M.; Huang, W.; Qian, H. Design, synthesis and biological evaluation of novel triazole-core reversal agents against P-glycoprotein-mediated multidrug resistance. *RSC advances* **2016,** *6* (31), 25819–25828. https://doi.org/10.1039/C6RA02405J.
35. Gao, Y.; Shi, W.; Cui, J.; Liu, C.; Bi, X.; Li, Z.; Huang, W.; Wang, G.; Qian, H. Design, synthesis and biological evaluation of novel tetrahydroisoquinoline derivatives as P-glycoprotein-mediated multidrug resistance inhibitors. *Bioorg. Med. Chem.* **2018,** *26* (9), 2420–2427. https://doi.org/10.1016/j.bmc.2018.03.045.
36. Guglielmo, S.; Lazzarato, L.; Contino, M.; Perrone, M. G.; Chegaev, K.; Carrieri, A.; Fruttero, R.; Colabufo, N. A.; Gasco, A. Structure–Activity Relationship Studies on Tetrahydroisoquinoline Derivatives:[4′-(6,7-Dimethoxy-3,4-dihydro-1*H*-isoquinolin-2-ylmethyl)biphenyl-4-ol](MC70) Conjugated through Flexible Alkyl Chains with Furazan Moieties Gives Rise to Potent and Selective Ligands of P-glycoprotein. *J. Med. Chem.* **2016,** *59* (14), 6729–6738. https://doi.org/10.1021/acs.jmedchem.6b00252.
37. Li, Y. S.; Zhao, D. S.; Liu, X. Y.; Liao, Y. X.; Jin, H. W.; Song, G. P.; Cui, Z. N. Synthesis and biological evaluation of 2,5-disubstituted furan derivatives as P-glycoprotein inhibitors for Doxorubicin resistance in MCF-7/ADR cell. *Eur. J. Med. Chem.* **2018,** *151*, 546–556. https://doi.org/10.1016/j.ejmech.2018.04.012.
38. Mairinger, S.; Wanek, T.; Kuntner, C.; Doenmez, Y.; Strommer, S.; Stanek, J.; Capparelli, E.; Chiba, P.; Müller, M.; Colabufo, N. A.; Langer, O. Synthesis and preclinical evaluation of the radiolabeled P-glycoprotein inhibitor [(11)C]MC113. *Nucl. Med. Biol.* **2012,** *39* (8), 1219–25. https://doi.org/10.1016/j.nucmedbio.2012.08.005.
39. Colabufo, N. A.; Berardi, F.; Cantore, M.; Perrone, M. G.; Contino, M.; Inglese, C.; Niso, M.; Perrone, R.; Azzariti, A.; Simone, G. M.; Paradiso, A. 4-Biphenyl and 2-naphthyl substituted 6,7-dimethoxytetrahydroisoquinoline derivatives as potent P-gp modulators. *Bioorg. Med. Chem.* **2008,** *16* (7), 3732–43. https://doi.org/10.1016/j.bmc.2008.01.055.
40. Wu, Y.; Pan, M.; Dai, Y.; Liu, B.; Cui, J.; Shi, W.; Qiu, Q.; Huang, W.; Qian, H. Design, synthesis and biological evaluation of LBM-A5 derivatives as potent P-glycoprotein-mediated multidrug resistance inhibitors. *Bioorg. Med. Chem.* **2016,** *24* (10), 2287–97. https://doi.org/10.1016/j.bmc.2016.03.065.
41. Payne, M.; Bottomley, A. L.; Och, A.; Hiscocks, H. G.; Asmara, A. P.; Harry, E. J.; Ung, A. T. Synthesis and biological evaluation of tetrahydroisoquinoline-derived antibacterial compounds. *Bioorg. Med. Chem.* **2022,** *57*, 116648. https://doi.org/10.1016/j.bmc.2022.116648.

42. Ramanivas, T.; Sushma, B.; Nayak, V. L.; Chandra Shekar, K.; Srivastava, A. K. Design, synthesis and biological evaluations of chirally pure 1,2,3,4-tertrahydroisoquinoline analogs as anti-cancer agents. *Eur. J. Med. Chem.* **2015,** *92*, 608–618. https://doi.org/10.1016/j.ejmech.2015.01.030.
43. Capilla, A. S.; Soucek, R.; Grau, L.; Romero, M.; Rubio-Martínez, J.; Caignard, D. H.; Pujol, M. D. Substituted tetrahydroisoquinolines: synthesis, characterization, antitumor activity and other biological properties. *Eur. J. Med. Chem.* **2018,** *145*, 51–63. https://doi.org/10.1016/j.ejmech.2017.12.098.
44. Sim, S.; Lee, S.; Ko, S.; Phuong Bui, B.; Linh Nguyen, P.; Cho, J.; Lee, K.; Kang, J. S.; Jung, J. K.; Lee, H. Design, synthesis, and biological evaluation of potent 1,2,3,4-tetrahydroisoquinoline derivatives as anticancer agents targeting NF-κB signaling pathway. *Bioorg. Med. Chem.* **2021,** *46*, 116371. https://doi.org/10.1016/j.bmc.2021.116371.
45. Wilson, R. J.; Jecs, E.; Miller, E. J.; Nguyen, H. H.; Tahirovic, Y. A.; Truax, V. M.; Kim, M. B.; Kuo, K. M.; Wang, T.; Sum, C. S.; Cvijic, M. E.; Paiva, A. A.; Schroeder, G. M.; Wilson, L. J.; Liotta, D. C. Synthesis and SAR of 1,2,3,4-Tetrahydroisoquinoline-Based CXCR4 Antagonists. *ACS Med. Chem. Lett.* **2018,** *9* (1), 17–22. https://doi.org/10.1021/acsmedchemlett.7b00381.

Information about the authors:
Maryam Amra Jordaan, Doctor of Philosophy, Research Directorate, Mangosuthu University of Technology; https://orcid.org/0000-0002-3057-123X.
Oluwakemi Ebenezer (*corresponding author*), Research Fellow, Department of Chemistry, Faculty of Natural Science, Mangosuthu University of Technology; https://orcid.org/0000-0003-1054-9665; e-mails for correspondence: re.korede@gmail.com, ebenezer.oluwakemi@mut.ac.za.

ISSN 2308-8303 (Print) / 2518-1548 (Online)